

Electronic supplementary Information

BaCo₄(OH)₂(H₂PO₄)(HPO₄)₂(PO₄): Archimedean Lattice T11 in Distorted Layers Built by Co₄O₁₂(OH)₄ Squares†

Wenbin Guo,^a Yingying Tang,^{a,b} Suyun Zhang,^a Sihuai Chen,^a Hongping Xiang^a, Jinqiu Xu,^{a,b} Meiyuan Cui,^{a,b} Lin Wang,^a Chaoqun Qiu^{a,b} and Zhangzhen He*,^a

a. State Key Laboratory of Structural Chemistry, Fujian Institute of Research on the Structure of Matter, Chinese Academy of Sciences, Fuzhou, Fujian 350002, P. R. China

b. University of the Chinese Academy of Sciences, Beijing, 100039, P. R. China

* To whom correspondence should be addressed.

E-mail: hezz@fjirsm.ac.cn

EXPERIMENTAL SECTION

1. Preparation of BaCo₄(OH)₂(H₂PO₄)(HPO₄)₂(PO₄) (1).

2. Energy-dispersive X-ray spectroscope.

3. X-ray Crystallography.

4. Magnetic measurements.

5. Thermal Analysis.

Figure S1. Topological relationship between Archimedean lattice T11 (left) and 1/5 depleted square lattice (right). The squares rotate 45° and octagons metamorphose into larger squares in 1/5 depleted square lattice.

Figure S2. (a, b) Three fold rotational symmetry in KFe₃(SO₄)₂(OH)₆ and BaFe₂(PO₄)₂ and (c, d) fourfold rotational symmetry in Li₂VOGeO₄ (X = Ge, Si) and PbZnVO(PO₄)₂.

Figure S3. (a) Photograph and (b) Energy-dispersive X-ray spectroscopy of **1**.

Figure S4. The Co···Co distances in a distorted octagon in {Co₄O₁₂(OH)₂}_∞ layer.

Figure S5. The coordination environments of (a) P(1)O₃(OH)²⁻, (b) P(2)O₃(OH)²⁻, (c) P(3)O₂(OH)₂⁻ and (d) P(4)O₄³⁻ in **1**.

Figure S6. The calculation and experiment powder of **1**.

Figure S7. TGA curves of **1**.

Figure S8. The temperature dependence of the magnetic susceptibility reciprocal for **1**.

Figure S9. The observed peaks in $\partial\chi/\partial T$ and $\partial\chi T/\partial T$ indicating the canted long-range ordering temperature of **1**.

Table S1. Crystal data and structure refinements for **1**.

Table S2. Selected bond distances, angles and VBS value of **1**.

Table S3. Atomic coordinates ($\times 10^4$) and equivalent isotropic displacement parameters ($\text{\AA}^2 \times 10^3$) for **1**.

Table S4. Anisotropic displacement parameters ($\text{\AA}^2 \times 10^3$) for **1**.

1 Preparation of BaCo₄(OH)₂(H₂PO₄)₂(HPO₄)₂(PO₄) (1).

BaCO₃, CoCl₂·6H₂O and C₂H₁₀N₆H₂CO₃ were analytically pure from Shanghai Reagent Factory (AR, 99.9%) and used without further purification. Synthesis of **1** was proceeded by the reaction of a mixture of 1 mmol BaCO₃ (3N, 0.3950 g), 2 mmol CoCl₂·6H₂O (3N, 0.9516 g), 2 mmol C₂H₁₀N₆H₂CO₃ (3N, 0.3632 g), 0.8 ml H₃PO₄(85%, 1.3480 g) and 10 mL H₂O in an autoclave equipped with a Teflon liner (28 mL) through a typical hydrothermal reaction at 170 °C for three days, yielding purple needle-shaped crystals of **1** (Figure S3a). The crystals were carefully selected, washed, dried. The quality of the samples was confirmed by powder XRD studies (Figure S6).

2 Energy-dispersive X-ray spectroscope.

Microprobe elemental analyses for the Ba, Co and P elements were performed on a field-emission scanning electron microscope (FESEM, JSM6700F) equipped with an energy-dispersive X-ray spectroscope (EDS, Oxford INCA). The EDS analysis of **1** confirms the Ba/Co/P/O elemental composition (Figure S3b).

3 X-ray Crystallography.

Single crystal of **1** was selected and mounted on glassy fibers for single crystal X-ray diffraction (XRD) measurements. Data collections were performed on Rigaku Mercury CCD diffractometer equipped with a graphite-monochromated Mo- K_{α} radiation ($\lambda = 0.71073 \text{ \AA}$) at 293 K. The data sets were corrected for Lorentz and polarization factors as well as for absorption by Multi-scan method^[1]. The structure was solved by direct methods and refined by full-matrix least-squares fitting on F^2 by *SHELX-97*^[2]. The final refined structural parameters were checked by the *PLATON* program^[3]. Crystallographic data and structural refinements for this compound are summarized in Tables S1-4. According to the bond valence calculations^[4], the calculated bond valences of O(1), O(2), O(3), O(12), and O(13) are 0.607, 1.035, 1.235, 1.221, and 1.263, respectively, while Co1, Co2, P1, P2, P3, P4 and other oxygen atoms in their ideal oxidation states (Table S2). Hence, O(1), O(2), O(3), O(12), and O(13) should be OH for charge balancing the formula.

4 Magnetic measurements.

For magnetic measurements, the crystal samples were ground. Magnetic measurements were

performed using a commercial Quantum Design Physical Property Measurement System (PPMS). Powder samples (9.46 mg) of **1** were placed in a gel capsule sample holder which was suspended in a plastic drinking straw. Magnetic susceptibility was measured at 0.1 T from 300 to 2 K (temperature scan of 5 K/min), and magnetization was measured at 2 K in applied field from 0 to 8 T (field scan of 0.1 T/step). Moreover, magnetic susceptibility was also measured with field-cooling (FC) and zero-field-cooling (ZFC) regimes under the field of 500 Oe from 2 to 30 K.

5 Thermal Analysis.

Thermogravimetric analysis (TGA) was performed with a Netzsch STA 449C instrument in a nitrogen atmosphere at a heating rate of $10\text{ }^{\circ}\text{C min}^{-1}$. The samples were placed in Al_2O_3 crucibles and heated from room temperature to $1000\text{ }^{\circ}\text{C}$. The weight loss between $300\text{ }^{\circ}\text{C}$ and $530\text{ }^{\circ}\text{C}$ is attributed to the loss of three H_2O molecules from the dehydration of OH^- groups^[5], (Figure S7) because the observed weight loss of 7.1% is close to the theoretical one 6.8% of **1**.

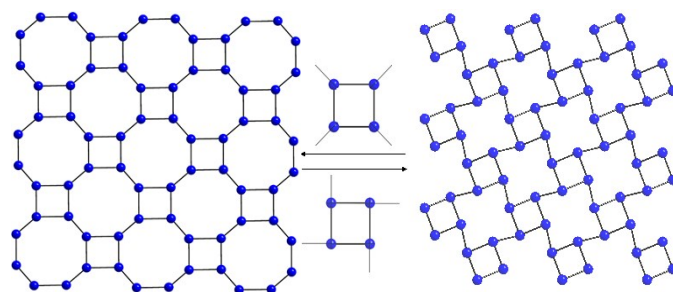


Figure S1. Topological relationship between Archimedean lattice T11 (left) and 1/5 depleted square lattice (right). The squares rotate 45° and octagons metamorphose into larger squares in 1/5 depleted square lattice.

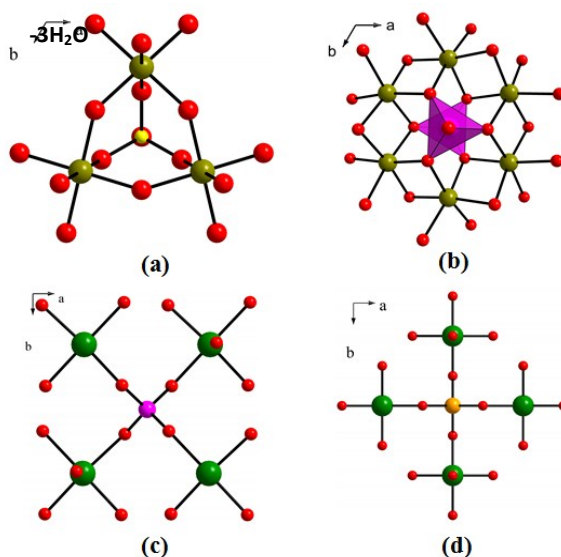


Figure S2. (a, b) Three fold rotational symmetry in $\text{KFe}_3(\text{SO}_4)_2(\text{OH})_6$ and $\text{BaFe}_2(\text{PO}_4)_2$ and (c, d) four fold rotational symmetry in $\text{Li}_2\text{VOGeO}_4$ (X = Ge, Si) and $\text{PbZnVO}(\text{PO}_4)_2$.

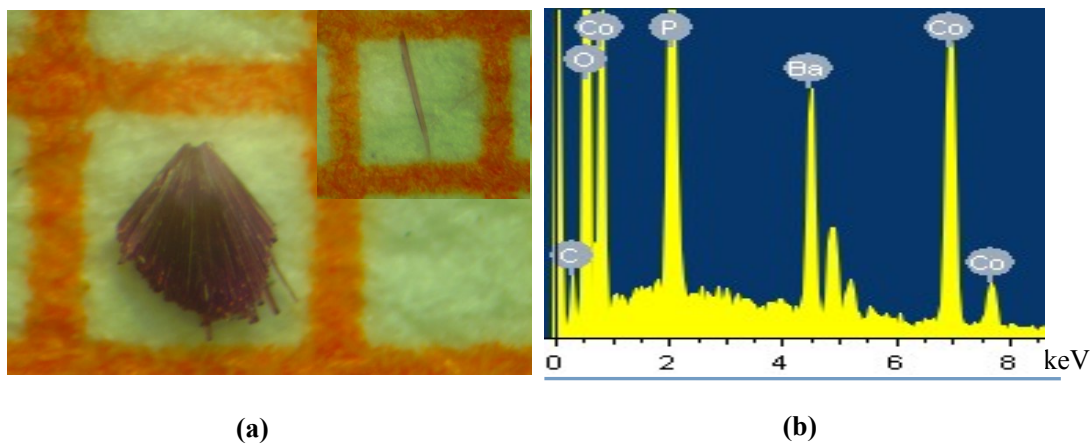


Figure S3. (a) Photograph and (b) Energy-dispersive X-ray spectroscopy of 1.

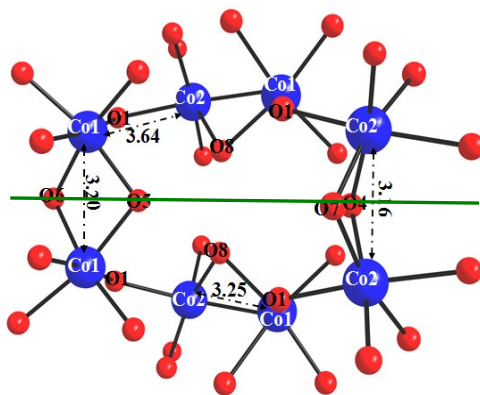


Figure S4. The Co \cdots Co distances in a distorted octagon of $\{\text{Co}_4\text{O}_{12}(\text{OH})_2\}_{\infty}$. The green line represents a mirror symmetry in the distorted octagon.

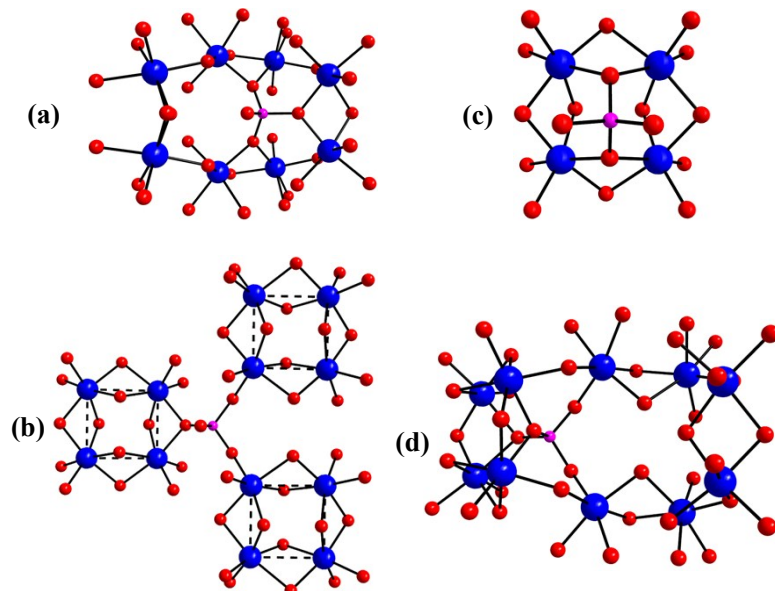


Figure S5. The coordination environment of (a) P(1)O₃(OH)²⁻, (b) P(2)O₃(OH)²⁻, (c) P(3)O₂(OH)₂⁻ and (d) P(4)O₄³⁻ in **1**.

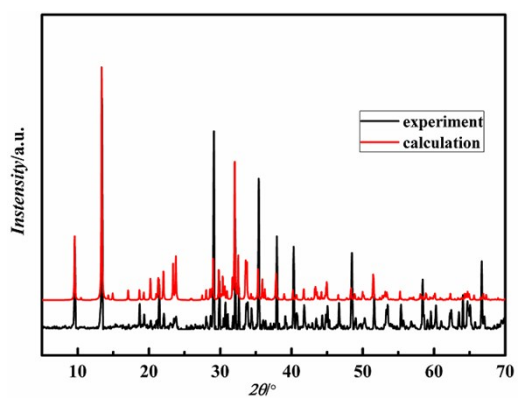


Figure S6. The calculation and experiment powder of **1**.

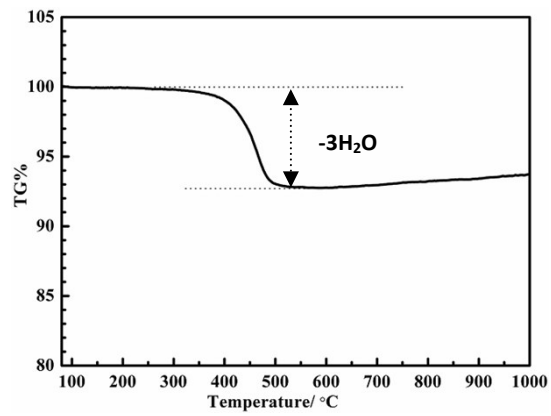


Figure S7. TGA curves of **1**.

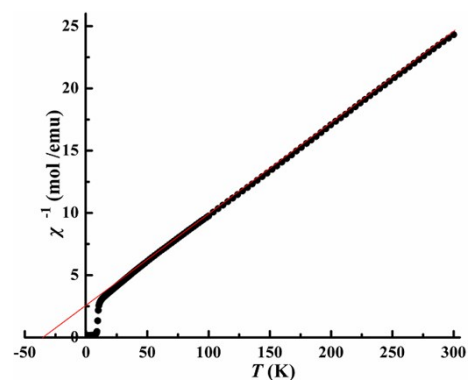


Figure S8. The temperature dependence of the magnetic susceptibility reciprocal for **1**.

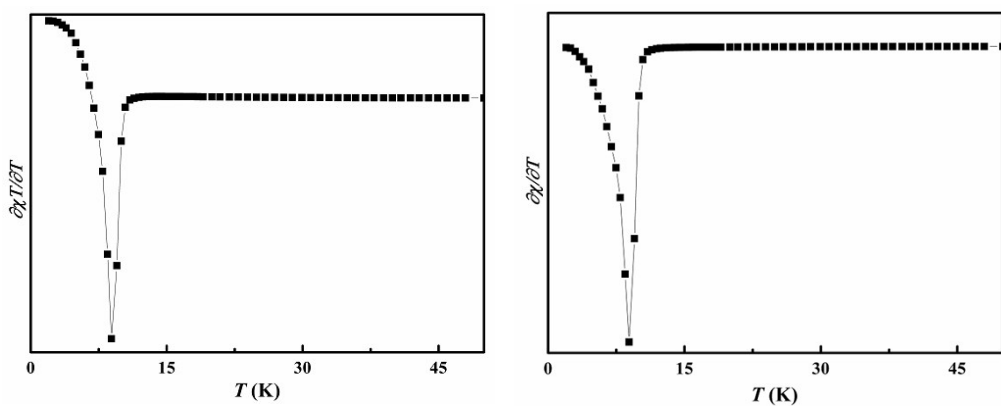


Figure S9. The sharp peaks in $\partial\chi/\partial T$ and $\partial\chi T/\partial T$ indicating the long-range ordering temperature of **1**.

Table S1. Crystal data and structure refinements for **1**.

formula	BaCo ₄ (OH) ₂ (H ₂ PO ₄)(HPO ₄) ₂ (PO ₄)
fw	790.99
T, K	room temp
λ, Å	0.71073
space group	<i>Pnma</i>
a, Å	18.453(2)
b, Å	8.3383(9)
c, Å	9.4995(1)
α, deg	90
β, deg	90
γ, deg	90
V, Å ³	1461.7(3)
Z	4
D _{calcd} , g cm ⁻³	3.567
μ, mm ⁻¹	7.640
Max. and Min. transmissions	1.0000, 0.7149
GOF on F^2	1.157
R1, wR2 [$I > 2\sigma(I)$] ^a	0.0492, 0.1112
R1, wR2 (all data)	0.0619, 0.1190

^aR1 = $\sum ||F_o| - |F_c|| / \sum |F_o|$, wR2 = $\{\sum w[(F_o)^2 - (F_c)^2]^2 / \sum w[(F_o)^2]^2\}^{1/2}$

Table S2. Selected bond distances, angles and VBS value of **1**.

Ba#4 -O(11)	2.875(5)	Ba-O(10)#2	2.790(5)
Ba-O(13)#8	2.902(6)	Ba-O(9)	2.996(5)
Ba-O(12)#8	2.907(7)	Ba-O(8)#2	3.001(5)
Co(1)-O(10)	2.048(5)	Co(1)-O(5)	2.051(4)
Co(1)-O(8)	2.090(5)	Co(1)-O(1)	2.156(4)
Co(1)#9-O(6)	2.188(5)	Co(1)-O(9)	2.239(5)
B.V.S.	1.876		
Co(2)-O(11)	1.986(5)	Co(2)-O(4)	2.037(4)
Co(2)-O(1)#2	2.124(5)	Co(2)-O(7)	2.126(4)
Co(2)-O(9)#3	2.205(5)	Co(2)-O(8)#3	2.270(4)
B.V.S.	1.923		
P(1)-O(5)#1	1.522(7)	P(1)-O(3)	1.538(6)
P(1)-O(8)#2	1.553(4)	P(1)-O(8)	1.553(4)
B.V.S.	4.904		
P(2)-O(7)#5	1.530(6)	P(2)-O(11)#6	1.533(5)
P(2)-O(11)	1.533(5)	P(2)-O(2)	1.604(7)
B.V.S.	4.813		
P(3)-O(12)	1.527(7)	P(3)-O(9)	1.539(5)
P(3)-O(9)#7	1.539(5)	P(3)-O(13)	1.591(8)
B.V.S.	4.819		
P(4)-O(10)#2	1.540(5)	P(4)-O(10)	1.540(5)
P(4)-O(6)	1.540(7)	P(4)-O(4)	1.544(6)
B.V.S.	4.901		
O1-Co1	2.156(2)	O1-Co2	2.124(3)
B.V.S.	0.807		
O2-P2	1.604(7)	B.V.S.	1.035
O3-P1	1.538(7)	B.V.S.	1.235
O12-P3	1.527(7)	O12#8-Ba	2.907(7)
B.V.S.	1.221		
O13-P3	1.591(8)	O13#8-Ba	2.902(6)
B.V.S.	1.263		
Angels (deg)			
O(10)-Co(1)-O(5)	97.2(2)	O(10)-Co(1)-O(8)	91.99(1)
O(5)-Co(1)-O(8)	167.4(2)	O(10)-Co(1)-O(1)	95.36(2)
O(5)-Co(1)-O(1)	90.2(2)	O(8)-Co(1)-O(1)	97.51(1)
O(10)-Co(1)-O(6)#1	168.1(2)	O(5)-Co(1)-O(6)#1	72.7(2)
O(8)-Co(1)-O(6)#1	99.0(2)	O(1)-Co(1)-O(6)#1	78.9(2)
O(10)-Co(1)-O(9)	85.65(1)	O(5)-Co(1)-O(9)	96.6(2)
O(8)-Co(1)-O(9)	75.45(1)	O(1)-Co(1)-O(9)	172.93(1)
O(6)#1-Co(1)-O(9)	101.4(2)	O(11)-Co(2)-O(4)	168.3(2)
O(11)-Co(2)-O(1)#2	96.28(1)	O(4)-Co(2)-O(1)#2	79.9(2)

O(11)-Co(2)-O(7)	95.55(1)	O(4)-Co(2)-O(7)	73.74(1)
O(1)#2-Co(2)-O(7)	93.0(2)	O(11)-Co(2)-O(9)#3	89.77(2)
O(4)-Co(2)-O(9)#3	96.5(2)	O(1)#2-Co(2)-O(9)#3	165.85(2)
O(7)-Co(2)-O(9)#3	99.2(2)	O(11)-Co(2)-O(8)#3	93.59(2)
O(4)-Co(2)-O(8)#3	97.70(2)	O(1)#2-Co(2)-O(8)#3	94.15(2)
O(7)-Co(2)-O(8)#3	167.73(2)	O(9)#3-Co(2)-O(8)#3	72.65(2)

B.V.S. = $\sum e^{(r_0-r)/b}$, with the following parameters: b=0.37, r0(Co-O)=2, r0(P-O)=2.

Symmetry transformations used to generate equivalent atoms: #1 -x+1/2, -y, z-1/2; #2 x, -y+1/2, z; #3 -x+1/2, y+1/2, z+1/2; #4 -x+1/2, -y+1, z+1/2; #5 -x, -y+1, -z+1; #6 x, -y+3/2, z; #7 x, -y-1/2, z; #8 -x+1, -y, -z+1.

Table S3. Atomic coordinates ($\times 10^4$) and equivalent isotropic displacement parameters ($\text{\AA}^2 \times 10^3$) for **1**. U(eq) is defined as one third of the trace of the orthogonalized U_{ij} tensor.

Atom	x	y	z	U(eq)
Co(1)	2719(1)	-581(1)	3748(1)	13(1)
Co(2)	1220(1)	4394(1)	6015(1)	14(1)
P(1)	2519(1)	2500	1662(3)	11(1)
P(2)	242(1)	7500	5209(3)	12(1)
P(3)	4292(1)	-2500	3847(3)	12(1)
P(4)	2716(1)	2500	5907(3)	11(1)
O(1)	1588(2)	21(5)	3960(5)	14(1)
O(2)	709(3)	7500	3786(7)	14(2)
O(3)	1761(3)	2500	2337(7)	14(1)
O(4)	1890(3)	2500	5642(7)	11(1)
O(5)	2580(4)	-2500	5071(7)	14(1)
O(6)	2787(4)	2500	7523(7)	16(1)
O(7)	549(3)	2500	5273(7)	14(1)
O(8)	2962(2)	1002(5)	2108(5)	16(1)
O(9)	3894(2)	-1001(6)	3299(6)	17(1)
O(10)	3073(2)	1017(5)	5235(5)	16(1)
O(11)	436(2)	6024(6)	6092(5)	16(1)
O(12)	5104(4)	-2500	3545(8)	19(2)
O(13)	4292(3)	-2500	5522(8)	20(2)
Ba	4184(1)	2500	3726(1)	16(1)

Table S4. Anisotropic displacement parameters ($\text{\AA}^2 \times 10^3$) for **1**. The anisotropic displacement factor exponent takes the form: $-2 \pi^2 [h^2 a^{*2} U_{11} + \dots + 2 h k a^* b^* U_{12}]$.

Atom	U11	U22	U33	U23	U13	U12
Co(1)	14(1)	11(1)	12(1)	0(1)	1(1)	0(1)
Co(2)	13(1)	11(1)	17(1)	0(1)	0(1)	1(1)
P(1)	10(1)	10(1)	12(1)	0	-1(1)	0
P(2)	11(1)	13(1)	13(1)	0	-2(1)	0
P(3)	10(1)	13(1)	13(1)	0	1(1)	0
P(4)	11(1)	13(1)	9(1)	0	0(1)	0
O(1)	13(2)	12(2)	16(3)	1(2)	0(2)	0(2)
O(2)	12(3)	19(3)	12(4)	0	2(3)	0
O(3)	10(3)	18(3)	14(4)	0	-2(3)	0
O(4)	5(3)	11(3)	16(4)	0	3(3)	0
O(5)	22(3)	10(3)	9(4)	0	2(3)	0
O(6)	17(3)	18(3)	12(4)	0	0(3)	0
O(7)	11(3)	13(3)	18(4)	0	-4(3)	0
O(8)	17(2)	13(2)	16(3)	3(2)	3(2)	6(2)
O(9)	16(2)	15(2)	20(3)	2(2)	4(2)	0(2)
O(10)	15(2)	19(2)	13(3)	-3(2)	1(2)	3(2)
O(11)	16(2)	14(2)	17(3)	3(2)	-1(2)	6(2)
O(12)	12(3)	27(4)	18(4)	0	-1(3)	0
O(13)	16(3)	32(4)	12(4)	0	-4(3)	0
Ba	13(1)	18(1)	16(1)	0	1(1)	0

References

- [1] *CrystalClear*, Version 1.3.5., Rigaku Corp., Woodlands, TX, **1999**.
- [2] G. M. Sheldrick, *Crystallographic Software Package, SHELXTL*, Version 5.1, Bruker-AXS, Madison, WI, **1998**.
- [3] A. L. Spek, *J. Appl. Crystallogr.*, **2003**, *36*, 7.
- [4] (a) I. D. Brown, D. Altermatt, *Acta Crys tallogr. B* **1985**, *41*, 244; (b) N. E. Brese, M. O'keeffe, *Acta Cryst allogr. B* **1991**, *47*, 192.
- [5] S. Vilminot, G. André, F. Bourée-Vigneron, M. Richard-Plouet, M. Kurmoo, *Inorg. Chem.* **2007**, *46*, 10079.